CXCR1 participates in bone cancer pain induced by Walker 256 breast cancer cells in female rats

Chengfei Xu[1,2], Baoxia Zhao[1], Longsheng Xu[1], Yahui Wang[1,3], Beibei Liu[1], Miao Xu[1], Qiuli He[1], Chaobo Ni[1], Jie Fu[1], Min Kong[1], Xuewu Lin[3], Huadong Ni[1] , and Ming Yao[1]

Abstract

Bone cancer pain (BCP) is a clinically intractable mixed pain, involving inflammation and neuropathic pain, and its mechanisms remain unclear. CXC chemokine receptor 1 (CXCR1, IL-8RA) and 2 (CXCR2, IL-8RB) are high-affinity receptors for interleukin 8 (IL8). According to previous studies, CXCR2 plays a crucial role in BCP between astrocytes and neurons, while the role of CXCR1 remains unclear. The objective of this study was to investigate the role of CXCR1 in BCP. We found that CXCR1 expression increased in the spinal dorsal horn. Intrathecal injection of CXCR1 siRNA effectively attenuated mechanical allodynia and pain-related behaviors in rats. It was found that CXCR1 was predominantly co-localized with neurons. Intrathecal injection of CXCR1-siRNA reduced phosphorylated JAK2/STAT3 protein levels and the NLRP3 inflammasome (NLRP3, caspase1, and IL-1β) levels. Furthermore, in vitro cytological experiments confirmed this conclusion. The study results suggest that the spinal chemokine receptor CXCR1 activation mediates BCP through JAK2/STAT3 signaling pathway and NLRP3 inflammasome (NLRP3, caspase1, and IL-1β).

Introduction

Bone cancer pain (BCP) is a severe cancer linked to metastatic lung, breast, and prostate cancers.[1] Approximately 75% of the patients experience moderate or severe pain, and more than half of them have no effective therapies for BCP.[2] Cancer pain increases patients' emotional distress, reduces their quality of life, and leads to an increase in mortality.[3] At present, there is a lack of therapeutic interventions, and the pathogenesis of the disease has not been fully understood.

According to previous studies, CXC chemokine receptor 2 (CXCR2, IL-8RB) plays a pivotal role in the interaction between astrocytes and neurons in BCP,[4] while the role of CXC chemokine receptor 1(CXCR1, IL-8RA) remains unclear. CXCR1/2 receptors are widely studied in tumors.[5] Moreover, the deletion of CXCR1 receptor probably increases the availability of CXCR1/2 ligands for CXCR2 binding.[6] CXCR1 and CXCR2 have different regulation in different brain regions, which means they may have different functions.[7] Studies have shown that CXCR2 plays a key role

[1]Department of Anesthesia and Pain Medicine, Affiliated Hospital of Jiaxing University, Jiaxing, China
[2]Department of Anesthesia, The Third People's Hospital of Bengbu, Bengbu, China
[3]Department of Anesthesia, The First Affiliated Hospital of Bengbu Medical College, Bengbu, China

Corresponding Authors:
Ming Yao, Department of Anesthesiology and Pain Research Center, The First Affiliated Hospital of Jiaxing University, 1882, Zhonghuansouth Road, Jiaxing 314001, China.
Email: jxyaoming666@163.com

Huadong Ni, Department of Anesthesiology and Pain Research Center, The First Affiliated Hospital of Jiaxing University, 1882, Zhonghuansouth Road, Jiaxing 314001, China.
Email: huadongni@126.com

in the induction and maintenance of inflammatory pain[8] and neuropathic pain,[9] and BCP facilitation.[4] In the rat neuropathic pain model induced by chemotherapy, CXCR1 is significantly upregulated compared to the control group.[10] However, it remains unclear whether CXCR1 is implicated in the development and maintenance of BCP.

JAK2/STAT3 pathway is implicated in inflammatory pain,[11] neuropathic pain,[12] and BCP.[13] NLRP3 inflammasome is also involved in the development and progression of BCP.[14,15] In addition, the activation of NLRP3 inflammasome is inhibited after the suppression of JAK2/STAT3 pathway.[16] However, it remains unknown whether NLRP3 inflammasome and JAK2/STAT3 pathway are implicated in BCP model.

We studied whether CXCR1 participated in the development of BCP through JAK2/STAT3 signaling pathway and NLRP3 inflammasome. We evaluated the expression of CXCR1 in the spinal dorsal horn of rats after Walker 256 cell injection. We further studied the expression of JAK2, p-JAK2, p-STAT3, STAT3, and NLRP3 inflammasome proteins in the spinal dorsal horn of rats in vivo.

Experimental protocol

Four parts of experiment protocol

Construction and validation of BCP model. The rats were randomly divided into naïve, sham, and BCP group ($n = 8$). Paw withdrawal threshold (PWT) was detected 1 day before operation and 6, 12, and 18 days after operation. The rats in Sham group and BCP group were detected with computed tomography (CT) and the bone tissue sections were hematoxylin and eosin (HE) 18 days after BCP operation ($n = 4$) (Figure 1(a)).

Detection of the expression of CXCR1, JAK2, p-JAK2, p-STAT3, and STAT3 and the distribution of CXCR1⁺ cells in the spinal cord of BCP rats. The rats randomly divided into sham and BCP (6, 12, 18 days) groups ($n = 4$). Sham and BCP (12 days) group rats were used for RT-PCR ($n = 8$) and immunofluorescence ($n = 4$) detection. The spinal cord of rats was stained with immunofluorescence. The tissues were co-labeled with GFAP (an astrocyte marker), NeuN (a neuronal marker), and Iba-1 (a microglial marker) (Figure 1(b)).

The relationship of BCP-induced hyperalgesia with CXCR1 and JAK2, p-JAK2, p-STAT3, STAT3, NLRP3, caspase1, and IL-1β expression. The rats were randomly divided into five groups: sham, BCP, BCP + si-control, and BCP + si-CXCR1 group ($n = 8$), PWT was detected 1 day before operation and 6, 12, and 18 days after operation. CXCR1 siRNA or missense siRNA was injected daily for 6 days from days 7–12 after surgery. Gait analysis ($n = 8$) was performed, and Western blot ($n = 4$)/ ELISA ($n = 3$) were performed on day 12 after the last drug administration (Figure 1(c)).
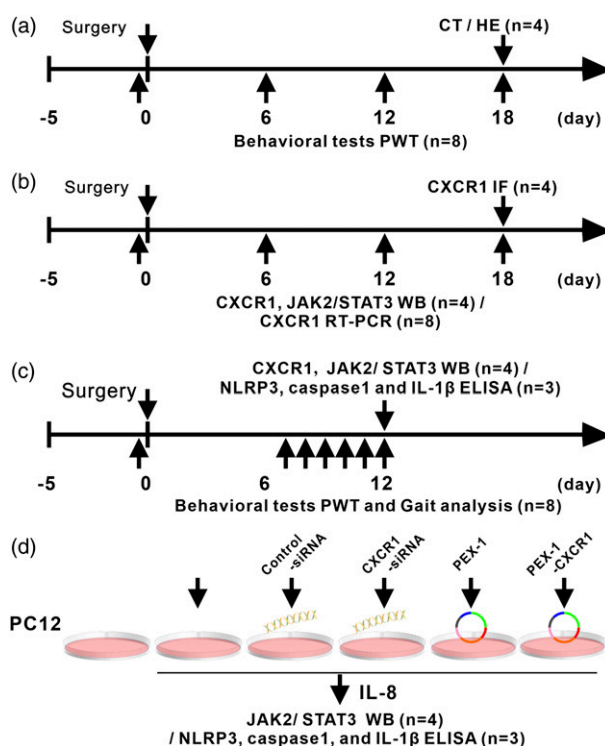

Figure 1. Experimental paradigms. CT: computed tomography; HE: Hematoxylin and eosin; IF: Immunofluorescence; RT-PCR: Quantitative Real-Time Polymerase Chain Reaction; IL-8: interleukin eight; JAK2: janus-activated kinase two; STAT3: signal transducer and activator of transcription three; PWT: paw withdrawal threshold; WB: Western blotting; ELISA: Enzyme-linked immunosorbent assay; PC12: PC12 cell lines.

The association of JAK2/STAT3 signaling pathway and NLRP3 inflammasome activation with CXCR1. PC12 cells were divided into six groups (treatment protocol is in Figure 1(d)), then JAK2, p-JAK2, p-STAT3, STAT3, NLRP3, caspase1, and IL-1β expression ($n = 3/4$) were detected.

Animals

The Experimental Animal Center of Zhejiang Province Academy of Medical Sciences, Hangzhou, China provided 180–200 g female Sprague-Dawley (SD) rats. They were kept at room temperature ($22 \pm 2°C$) in a 12 h light/dark cycle with enough food and water. Six to eight rats were housed per cage. All experiments were carried out in our laboratory during the day. Every attempt was made to reduce the utilized animals' number and suffering. The Animal Care Committee at Jiaxing University and the ethical instructions were followed for the pain examination experiments.[17]

BCP model

As in our previous studies,[18] rats (excluding the naïve group) were anesthetized with 50 mg/kg intraperitoneal sodium pentobarbital. A sterile incision was made in the lower third of the left leg and a hole was drilled. The bone medullary canal was slowly inoculated with Walker 256 breast cancer cells (10 µL, 1×10^6/mL) (BCP group) or heat-killed Walker 256 breast cancer cells (10 µL, 1×10^6/mL) (sham group). A fixed micro-syringe was used to prevent cell leakage for 2 min. The inoculation site was immediately sealed with bone wax.

CT reconstruction

CT imaging was initiated 12 days after tumor inoculation to confirm the development of tibial tumor. For 3D CT bone reconstruction, a CT scanner (SOMATOM, Siemens, Germany) was used. Regarding the previous study,[19] the CT scanner parameters were set as follows: 120 kVp, helical scanning, 1 mm layer thickness, 1 mm layer interval, Care dose 4D technique, high-resolution SD rat's tibia CT imaging (100 mm view field), and kernel: U30u medium smooth. The Siemens Syngo MultiModality Workplace (MMWP) post-processing workstation was employed to process and analyze the images.

Behavioral assessment using the Von Frey test

Mechanical allodynia was quantified via ipsilateral hind paw withdrawal from von Frey monofilaments (BME-404; Biological Medicine Institute, Medical Science Academy, Beijing, China), as we stated before.[18] Three days before the experiment, all rats were handled to familiarize themselves with the test environment daily. The rats were allowed to acclimate to the transparent Plexiglas compartments ($25 \times 20 \times 20$ cm) for 30 min before each session. PWT measurements were repeated five times every 10 s and averaged. All behavioral assessments were done by researchers, who are blind to the experimental groups.

Catwalk automatic gait analysis

Gait analysis was utilized to measure pain-associated behaviors.[20] It tracks and assesses the rodents' voluntary movements in a closed pathway. A high-speed camera placed beneath the glass floor captured every paw parameter. We collected valid data, including at least four serial step cycles or complete tunnel passages. These parameters often used to assess pain-related behaviors were area and intensity data. In the current research, we employed three parameters for BCP-related behaviors evaluation: (1) "Max contact area" is the maximum hind paw contact area; (2) "Mean intensity" is the hind paw intensity average; (3) "Max contact max intensity" is the maximum intensity during maximum hind paw contact. To exclude the influence of confounding factors, we used left hind paw/right hind paw (LH/RH) to accurately illustrate the area and intensity data alterations.

Histological analysis of bone sections

After the rats were sacrificed, the ipsilateral tibia was excised and preserved in 4% paraformaldehyde. Tibia was demineralized in 10% EDTA for 1 day, and put in paraffin for histological analysis. Paraffin pieces were cut 8 µm thick sections on the coronal plane and stained with Hematoxylin and Eosin (H & E). All pictures were captured with a ×20 or ×40 objective by an Olympus B × 51 microscope usage.[21]

Cell culture, siRNA, and plasmid transfection

PC12 cells (the Chinese Academy of Sciences Cell Bank, China) were cultured in RPMI-1640 enriched with 1% antibiotics and 10% fetal bovine serum (FBS) in a humidified CO_2 incubator at 37°C, according to the manufacturer's recommendations. CXCR1-specific siRNA and control siRNA sequences were designed by RuiBo Biological Technology Co., Ltd (Guangzhou, China). The PEX-1-CXCR1 overexpression plasmid was provided by the Genepharma (Shanghai, China). PC12 cells were extracted in the log phase and seeded into 6-well plates (3×10^5/well). Two hours before the transfection, the cells were fed with a serum-free 1640 medium. The CXCR1 siRNA or CXCR1 over-expression plasmid (PEX-1-CXCR1) was transfected into PC12 cells with Lipofectamine 2000 (Invitrogen, # 1168019), and then treated with IL-8 (1 µg/mL). After the specified incubation time, the culture medium is collected and tested.

Intrathecal siRNA transfection

CXCR1-specific siRNA and Control siRNA sequences were designed by Guangzhou RuiBo Biological Technology Co., Ltd. The validated siRNA sequence is CXCR1: 5′-CTAACCTGGTTCACAAGGA -3′. The rats were subclassified into four groups ($n = 8$): sham, BCP, BCP + si-CXCR1 and BCP + si-control, CXCR1 siRNA (33 µg in 15 µL) or negative control siRNA were transfected via i.t. Injection on days 7–12 after tumor implantation. For intrathecal siRNA transfection, PE10 (0.28 mm inner diameter and 0.61 mm outer diameter) tubing was implanted in rats using L4/L5 lumbar approach as previously described.[22] The rats were then singly housed and remained on their respective diets throughout the experiment.

Western blot

The rats were administered a 4% pentobarbital sodium for anesthesia. Then, the ipsilateral spinal cord L3-L5 segments

were harvested. Tissues were lysed using RIPA buffer containing protease and phosphatase inhibitor cocktails, and then were homogenized with an ultrasonic homogenizer. The supernatant was centrifuged at 14,000 r/min at 4°C for 20 min. The protein concentration was determined using a BCA kit (Jiangsu Biyuntian Biotechnology Institute, Nantong, China). A 40 μg protein was loaded onto 10% SDS-polyacrylamide gel for electrophoresis and then separated proteins were transferred onto polyvinylidene difluoride membranes (PVDF) membranes by electroblotting. After two-hour blocking at room temperature, the membrane was incubated with a primary antibody at 4°C overnight in 5% nonfat milk. The secondary antibody was incubated at room temperature for 2 h. The enhanced chemiluminescence method and X-ray film were used for visualizing the protein bands. These primary antibodies were utilized for Western blotting (all at 1:1000 unless otherwise indicated): CXCR1 (bs-1009R, Bioss), p-JAK2 (CST #3771, Cell Signaling), JAK2 (CST #3230, Cell Signaling), p-STAT3 (AF3293, Affinity), STAT3 (10253-2-AP, Proteintech), and GAPDH (AF7021, Affinity). The target protein band intensity was quantified by ImageJ and normalized to GAPDH band.

Quantitative real-time polymerase chain reaction

The Trizol reagent was used extract the total RNA from the L3-5 spinal cord. The PrimeScript RT reagent kit was used to convert 1 μg of total RNA to cDNA, which was amplified utilizing these primers: CXCR1 forward, 5′-CCGTTCTGGAACAGTCTGCTATGAG-3′; CXCR1 reverse, 5′-ATGATGAACAGCGGCAAGAGGAAG-3′; CXCR2 forward, 5′-TGGTCCTCGTCTTCCTGCTCTG -3′; CXCR2 reverse, 5′-CGTTCTGGCGTTCACAGGTCTC -3′; β-actin forward, 5′-ATCACTATCGGCAATGAGCGGTTC-3′; β-actin reverse, 5′-TGTTGGCATAGAGGTCTTTACGGATG -3′. The PowerUp SYBR Green Master Mix was utilized for all PCR reactions performed on the StepOnePlus machine. The PCR amplifications were performed at 50°C and 95°C for 2 min, then 45 cycles at 95°C and 60°C for 15 s. To validate PCR product specificity in each well, melting curves were made. CXCR1 relative expression levels were determined by the comparative Ct method ($2^{-\Delta\Delta Ct}$ method).

Enzyme-linked immunosorbent assay (ELISA)

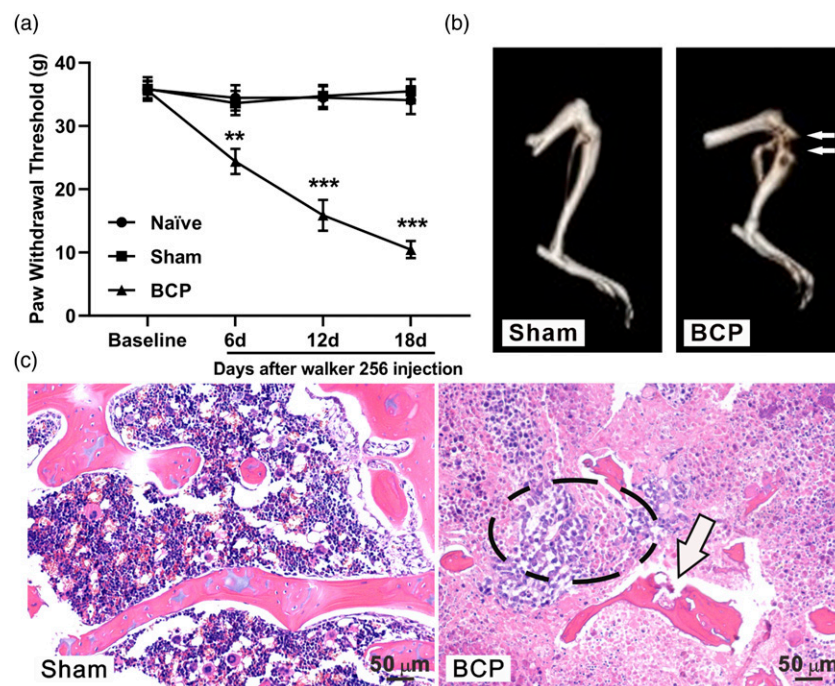Rat IL-1β ELISA Kit (Elabscience, Houston, TX, USA), rat NLRP3 and rat caspase1 ELISA Kits (USCNK, Wuhan,

Figure 2. Intratibial inoculation of Walker 256 cells produces bone destruction and progressive hyperalgesia. (a)The paw withdrawal threshold (PWT) of the ipsilateral hind paw was significantly decreased on BCP from 6 to 18 days after surgery. **$p < 0.01$ versus sham; ***$p < 0.001$ versus sham; $n = 8$, two-way repeated-measures ANOVA. (b) Three-dimensional (3D) reconstruction of CT scan showing marked bone destruction of the left tibia 18 days after tumor cell injection. Arrows point to cortical destruction sites. $N = 4$. (c) Representative images of hematoxylin-eosin staining showing that the bone marrow cavity of rats in the sham-operated group was filled with lymphocytes and macrophages. Trabecular surface cancer cell infiltration and bone resorption pits appeared in the bone marrow cavity of the tibia 18 days after tumor cell inoculation. $N = 4$. Scale bar: 50 μm.

China) were used. Rat spinal cord tissues were homogenized, and cultured cells were lysed in RIPA buffer containing protease and phosphatase inhibitors. The protein concentrations were identified using the BCA Protein Assay (Jiangsu Biyuntian Biotechnology). After protein quantitation, 100 μg protein was subjected to NLRP3, IL-1β, and caspase1 assay by ELISA following the manufacturer protocol.

Immunofluorescence

The rats were deeply anesthetized 12 days after BCP and then were perfused and fixed with 4% formaldehyde. For 6 h, spinal cords at the lumbar enlargement were immediately extracted and postfixed with 4% formaldehyde. The spinal cords were then dehydrated in 15% and 30% gradient sucrose solutions at 4°C for 2 days. The spinal cords were cut after being embedded in OTC compound into 16 μm sections, which were washed in PBS, and then blocked for 1 h using 10% normal goat serum. Next, sections were treated with primary antibodies at 4°C overnight and subsequently treated with fluorescent conjugated secondary antibodies at room temperature for 50 min. Nuclei were counterstained with DAPI (Invitrogen). Pictures were captured by a confocal laser microscope. The following primary antibodies were used: CXCR1 (1:100, bs-1009R, Bioss), NeuN (1:400, NBP1-92693, NOVUS), Iba-1 (1:300, ab5076, Abcam), and GFAP (1:400, C9205, Sigma). To confirm the specificity of the CXCR1 antibody, the CXCR1 antibody was pre-adsorbed (room temperature, 1 h) against its blocking peptide (bs-1009P, Bioss) prior to incubation with spinal cord sections, by mixing the CXCR1 antibody with a ten-fold (by weight) of
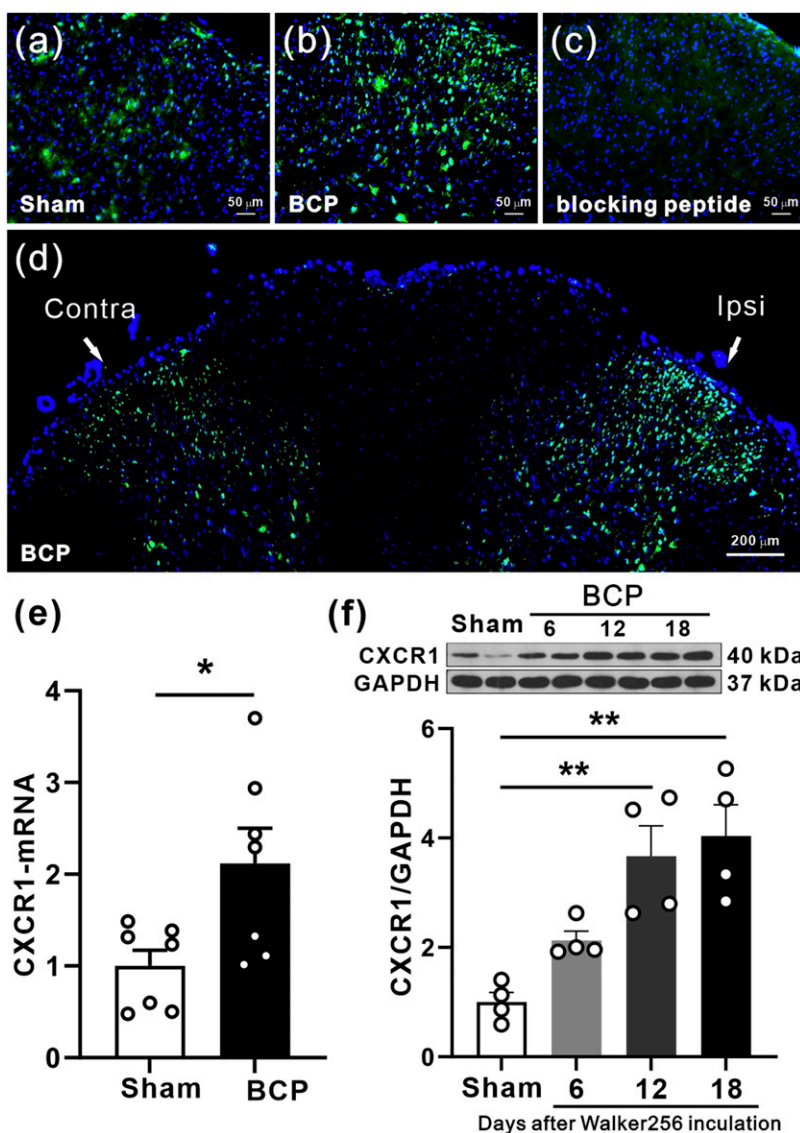

Figure 3. Increased CXCR1 protein and mRNA expression in the spinal dorsal horn of BCP rats. (a–d) Immunolabeled CXCR1 (green) in the spinal cord of BCP rats. Pre-incubation of CXCR1 antibody with excessive CXCR1 blocking peptide served as the specificity control of CXCR1 antibody. Ipsilateral (Ipsi), contralateral (Contra), nucleus (blue). (e) The mRNA expression of CXCR1 was increased in the BCP group compared with the sham group. *$p < 0.05$, $n = 7$, compared to sham, Student's t-test. (f) The protein expression of CXCR1 increased in a time-dependent manner in the BCP group compared with the sham-operated group. **$p < 0.01$; $n = 4$, one-way ANOVA.

the blocking peptide. The following secondary antibodies were used: 488 donkey anti-rabbit (1:500, ab150073, Abcam), 594 donkey anti-mouse (1:500, ab150108, Abcam), and 594 donkey anti-goat (1:500, ab150132, Abcam).

Quantification and statistics

All data were reported as mean ± SEM. Sample sizes were determined according to previous study. The one-way ANOVA and post hoc Dunnett multiple comparison tests were utilized to determine Catwalk gait results and the group differences for immunofluorescence experiments, Western blot, and RT-PCR. The two-way repeated-measures ANOVA and post hoc Bonferroni multiple comparison tests were utilized for determining the behavioral pain experiment. GraphPad Prism 6.0 software (GraphPad, San Diego, CA) was utilized to conduct all statistical analyses. $p < 0.05$ was considered statistically significant.

Results

Walker 256 cells inoculated into tibia causes bone destruction and progressive hyperalgesia

We used the rat model of BCP established by Mao Ying et al.[23] which was prepared by injecting Walker 256 breast cancer cells into the left tibia of SD rats. Consistent with our previous study,[21] mechanical allodynia occurred in the ipsilateral hind limb within 6 days after tumor inoculation and

lasted for 18 days (Figure 2(a)). To verify BCP model, we performed 3D CT imaging of the rat tibia 18 days after the inoculation of Walker 256 cells to assess the bone destruction (Figure 2(b)). The control animal treated with heat-inactivated tumor cells did not cause any distinctive changes. We then analyzed the structure of rat tibia in H & E staining of tissue sections (Figure 2(c)). In the sham group, naked nuclear lymphocytes, normal trabecular structures, and macrophages were apparent in the tibial bone marrow cavity of sham rats. However, in the BCP model, cancer cell infiltration and bone resorption pits were formed in the rat bone marrow cavity 18 days later.

CXCR1 expression and cellular localization in rat spinal cord

We detected CXCR1 protein expression and subcellular localization the expression and subcellular localization of CXCR1 protein in the spinal cord dorsal horn of rats. First, we used immunofluorescence to detect the expression and cellular localization of CXCR1 protein. To ensure the high specificity of CXCR1 antibody, the CXCR1 antibody was pre-adsorbed on its blocking peptide. After the CXCR1 primary antibody was pre-incubated with the blocking peptide, the treatment abrogated the detection of CXCR1 by immunofluorescence assay (Figure 3(c)). Clearly, compared with the sham operation group, the BCP group had significant changes (Figure 3(a) and (b)). The expression of CXCR1 was mainly distributed in the dorsal horn of the ipsilateral spinal
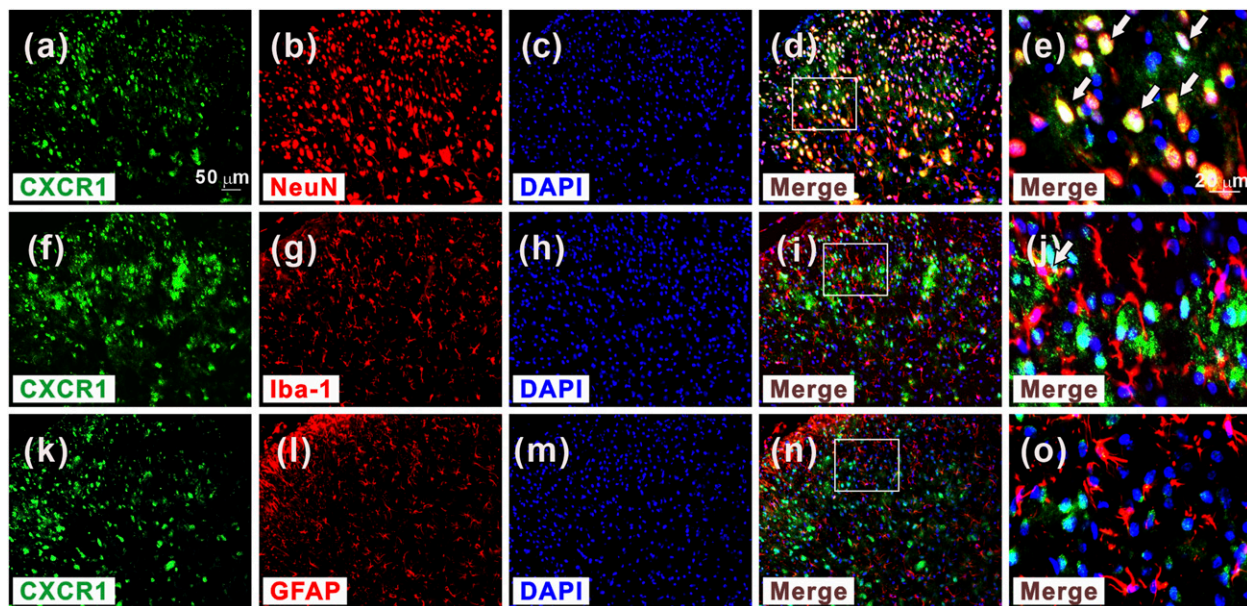

Figure 4. Distribution and cellular localization of CXCR1 in the dorsal horn of the spinal cord. (a–o) Immunofluorescence data show that CXCR1 (green) was predominantly expressed in neurons (red), but not in astrocytes (red) or microglia (red). All sections were counterstained with DAPI (blue) to show nuclei. White arrows indicate possible colocalization sites. NeuN (neuronal nucleus, neuron-specific marker); GFAP (glial fibrillary acidic protein, astrocyte-specific marker); Iba-1 (ionized calcium-binding adaptor molecule 1, microglia-specific mark); $n = 4$. Scale bar: 50 μm.
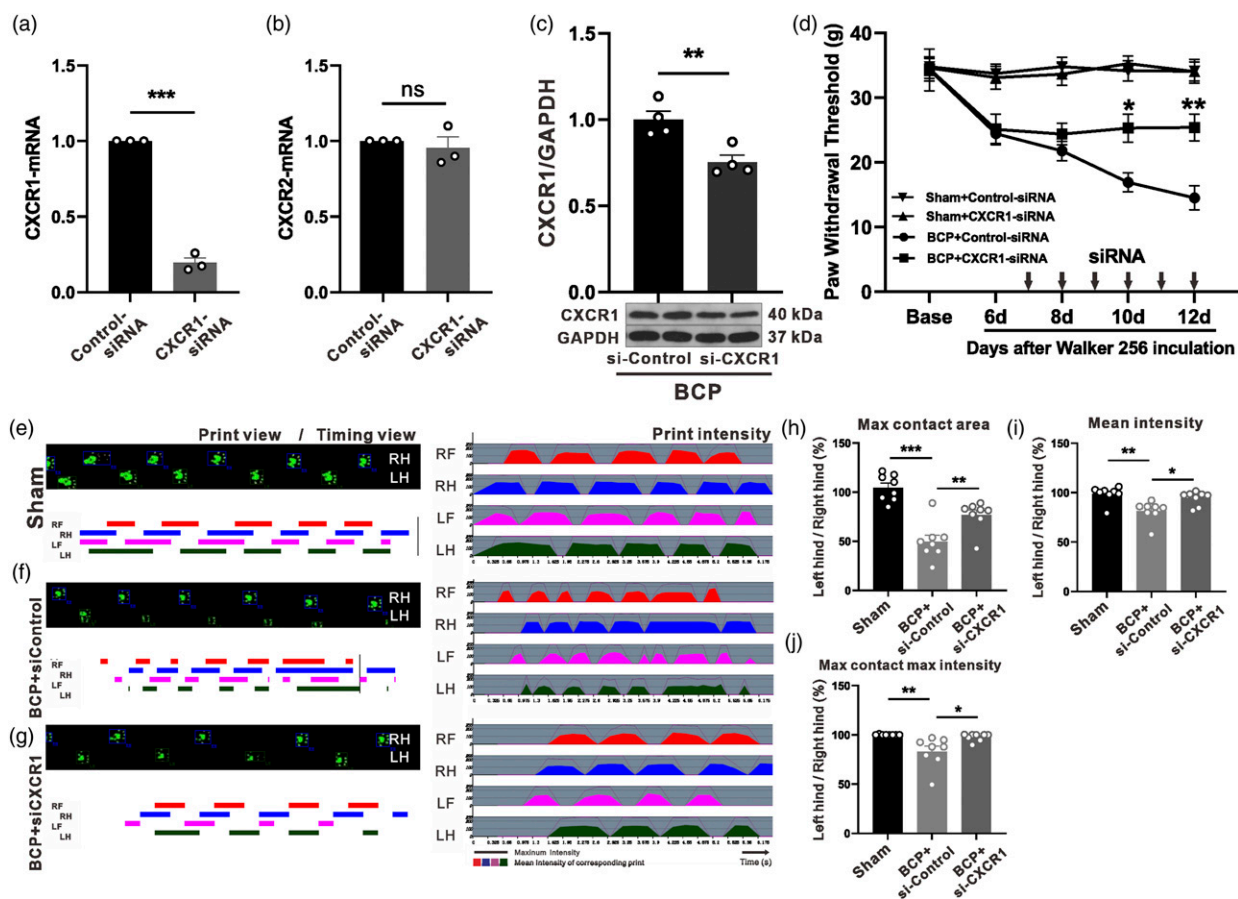
Figure 5. Spinal cord blockade of CXCR1 attenuates abnormal gait and mechanical hyperalgesia in BCP rats. (a-b) Relative expression of CXCR1-mRNA and CXCR2-mRNA in PC12 cells after CXCR1-siRNA transfection. ***$P < 0.001$. n = 3, Student's t-test. (c) Western blot results showing the reduction of CXCR1 protein levels after CXCR1-siRNA treatment. **$p < 0.01$. n = 4, Student's t-test. (d) Intrathecal injection of CXCR1-siRNA relieved tumor-induced mechanical allodynia 10 days after BCP. *$p < 0.05$, **$p < 0.01$, compared to sham, two-way repeated measures ANOVA. (e-g) Representative CatWalk gaits, including print view, timing view, and print intensity, in sham (e), BCP+siControl (f), BCP + si-CXCR1 (g) groups. (h-j) Intrathecal injection of CXCR1-siRNA significantly attenuated tumor-induced reductions in maximum contact area (h), maximum contact maximum intensity (j), and mean intensity (i) in tumor-bearing rats. Starting on day 7 after tumor inoculation, CXCR1-siRNA was intrathecally injected daily for six consecutive days. Behavioral testing was performed 4 h after the last injection. Data were calculated as percentages of ipsilateral (left)/contralateral (right) hind paws. Data are presented as mean ± SEM *$p < 0.05$, **$p < 0.01$, ***$p < 0.001$, one-way ANOVA. LH, left rear; RH, right rear.

cord on the inoculated side (Figure 3(d)). To determine the predominant cell types expressing CXCR1, we used cell type specific markers for double immunofluorescence staining: NeuN for neurons (Figure 4(a)–(e)), Iba-1 for microglia (Figure 4(f)–(j)), and GFAP for astrocytes (Figure 4(k)–(o)) on day 12 after BCP model. Notably, CXCR1 expression was mostly co-localized with neurons. Next, CXCR1 mRNA in BCP group increased compared to the sham group (Figure 3(e)). Western blot analysis results revealed that BCP induced CXCR1 protein expression to increase from the 6th to 18th day after BCP (Figure 3(f)). CXCR1 expression increased significantly on the 12th and 18th days. However, the increase on day 6 was not statistically significant.

Downregulation of CXCR1 alleviates the mechanical allodynia in BCP rats

Chemokine receptors are associated with activation of spinal neurons and glial cells during BCP.[24] To determine whether the upregulation of CXCR1 in the spinal dorsal horn was implicated in BCP, we tested whether the downregulation of CXCR1 by siRNA can alleviate hyperalgesia. In PC12 cells, CXCR1 siRNA significantly downregulated the expression of CXCR1 mRNA without affecting CXCR2 expression (Figure 5(a) and (b)). CXCR1-siRNA or control-siRNA was administrated intrathecally to rats for 6 days starting from the seventh day following Walker 256 cell injection. Western Blot results showed that intrathecal injection of CXCR1-
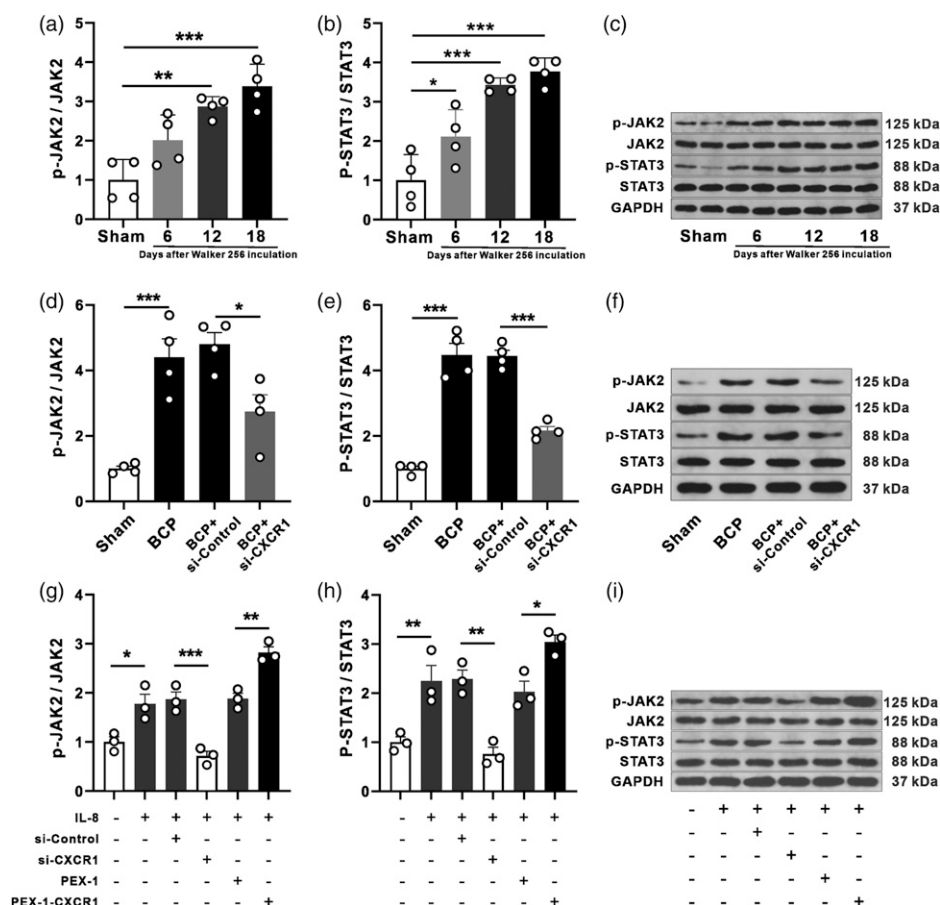
Figure 6. BCP-induced activation of spinal JAK2/STAT3 signaling is dependent on CXCR1 in vivo and in vitro. (a–c) The phosphorylated proteins of the JAK2/STAT3 pathway were time-dependently increased in the spinal cord of rats with BCP. *$p < 0.05$, **$p < 0.01$, ***$p <$ 0.001, compared to sham group, one-way ANOVA. (d–f) Phosphorylated proteins of the JAK2/STAT3 pathway were reduced after intrathecal injection of CXCR1-siRNA. *$p < 0.05$, ***$p < 0.001$, compared to sham group, one-way ANOVA. (g–i) Phosphorylated protein of JAK2/STAT3 was dependent on CXCR1 activation in PC12 cells. *$p < 0.05$, **$p < 0.01$, ***$p < 0.001$.

siRNA significantly reduced CXCR1 protein levels (Figure 5(c)). PWT and gait were recorded after intrathecal injection of CXCR1-siRNA and results showed that intrathecal injections of CXCR1-siRNA significantly increased PWT on the 10th day after modeling while control-siRNA administration had no effect on PWT. There was no statistically significant change in PWT in Sham+CXCR1-siRNA group, indicating that CXCR1 inhibition has no analgesic effect on basal pain (Figure 5(d)).

Gait analysis was utilized to measure pain-related behaviors. To comprehensively analyze the effects of BCP on ipsilateral and contralateral hind paws, we selected three parameters in rats: (1) maximum contact area, (2) mean intensity, and (3) maximum contact intensity. We adopted the criteria described by Yan-Qing Wang et al.,[25] percentages of ipsilateral (left)/contralateral (right) hind paw ratio. Compared with Sham group (Figure 5(e)), the maximum contact area, mean intensity, and percentage of maximum contact intensity of BCP⁺ control-siRNA group decreased significantly (Figure 5(f)). However, continuous intrathecal injection

of CXCR1-siRNA (Figure 5(g)) can significantly reverse tumor-induced gait (Figure 5(h)–(j)).

BCP-induced JAK2/STAT3 activation depends on CXCR1

JAK2/STAT3 signaling pathway is involved in BCP.[13] In our experiment, the expression of phosphorylated proteins of JAK2 and STAT3 was significantly increased, but total expression of JAK2 and STAT3 expressions was unchanged, which was consistent with our previous observation.[19] As shown in Figure 6(a)–(c), the levels of p-JAK2 and p-STAT3 in the spinal cord increased significantly from day 12 to day 18 after modeling. Previous reports indicate that CXCR1/2 could activate JAK2/STAT3 pathway.[26] We examined whether the activation of JAK2/TAT3 under BCP conditions depends on CXCR1. After 6 days of BCP modeling, CXCR1-siRNA or control-siRNA was injected intrathecally for six consecutive days. As shown in Figure 6(d)–(f), compared with the control group, CXCR1-siRNA significantly reduced
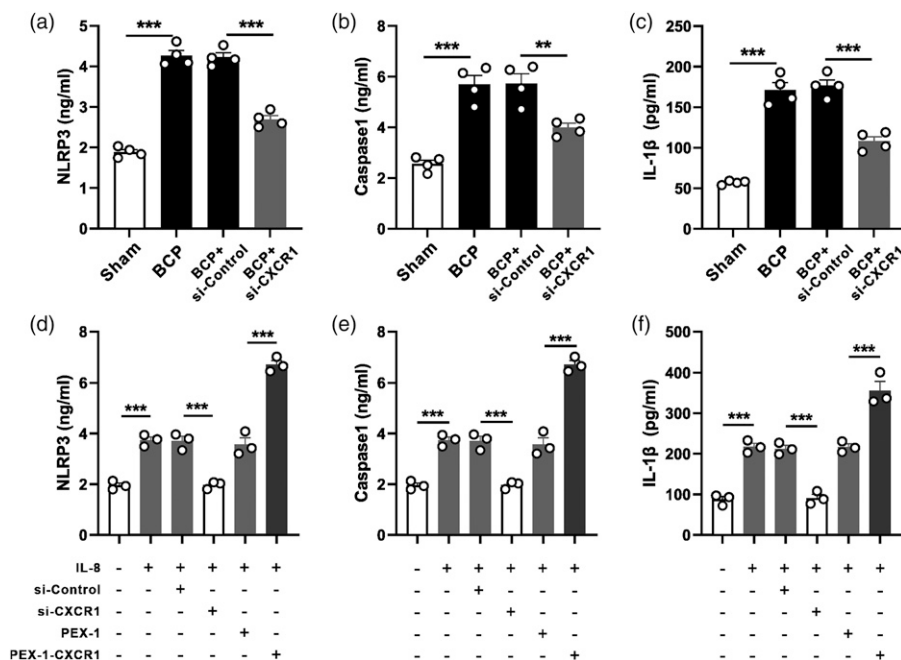
Figure 7. BCP-induced activation of the NLRP3 inflammasome is dependent on CXCR1 in vivo and in vitro. (a–c) Elevated NLRP3, caspase1, and IL-1β proteins in BCP rats were reversed after intrathecal injection of CXCR1-siRNA. **$p < 0.01$, ***$p < 0.001$, $n = 4$. (d–f) Increased protein level in NLRP3, caspase-1, and IL-1β was dependent on CXCR1 in PC12 cells. ***$p < 0.001$, $n = 3$.

p-JAK2 and p-STAT3 protein levels, but had no effect on their total protein level.

To further verify whether CXCR1 level regulates the activation of JAK2/STAT3 signaling pathway, we conducted in vitro experiments. As IL8 is a high-affinity ligand for CXCR1,[27] we used IL8 to activate CXCR1 receptor to mediate the downstream signaling pathways in PC12 cell line.[28] After IL8 treatment, p-JAK2 and p-STAT3 in PC12 cells increased significantly, especially after transfection with CXCR1 overexpression plasmid (Figure 6(g)–(i)). The results revealed that the activation of JAK2/STAT3 depended on CXCR1, which was consistent with our hypothesis. In vivo and in vitro experiments showed that CXCR1 receptor played a crucial role in BCP through JAK2/STAT3 signaling pathway.

BCP-induced activation of NLRP3 inflammasome depends on CXCR1

The activation of NLRP3 inflammasome contributes to the pathogenesis of inflammatory pain,[29] neuropathic pain,[30] and BCP.[31] Studies have indicated that MCC950 (NLRP3 inflammasome inhibitor) inhibits the activation of NLRP3 inflammasome and suppresses caspase-1-dependent processing of IL-1β. Similarly, MCC950 injection can attenuate BCP related mechanical pain hypersensitivity. Next, we examined whether the activation of NLRP3 inflammasome under BCP conditions relies on CXCR1. After modeling, compared with sham operation group, NLRP3/caspase-1/IL-

1β protein expression levels were considerably elevated. After intrathecal injection of CXCR1-siRNA, these proteins also decreased significantly (Figure 7(a)–(c)).

We further verified whether CXCR1 affected the level of NLRP3 inflammasome in PC12 cell line. CXCR1/2 antagonist G31P reduced the activation of NOD-like receptors protein 3 (NLRP3).[32] We also used the PC12 cell line to validate the role of CXCR1 with inflammasome. After treating PC12 cells with IL8, NLRP3 inflammasome (NLRP3, caspase-1 and IL-1β) were considerably elevated. This phenomenon can be reversed by CXCR1-siRNA. After PC12 cells were treated with IL-8, NLRP3 inflammasome (NLRP3, caspase-1 and IL-1β) were considerably elevated (Figure 7(d)–(f)) and this phenomenon can be reversed by CXCR1-siRNA. These outcomes indicate that CXCR1 receptor plays an important role in NLRP3 inflammasome.

Discussion

The main findings of this study were as follows: (1) after the tibia was injected with Walker-256 cells, the mechanical hyperalgesia threshold of rats was reduced, accompanied by a time-dependent increase in the ipsilateral spinal cord CXCR1, p-JAK2, p-STAT3, and NLRP3 inflammasome; (2) CXCR1 receptors were mainly co-located with neurons, which was different from previous studies[7]; (3) intrathecal injection of CXCR1-siRNA can reduce mechanical hyperalgesia and improve BCP-related behaviors; (4) Inhibition of CXCR1 in spinal cord can reduce p-JAK2, p-STAT3 activation and

NLRP3 inflammasome. These findings suggest that the activation of NLRP3 inflammasome, p-STAT3, and p-JAK2 in the spinal cord is an important mechanism of CXCR1 signaling in the development of BCP in rats.

BCP includes inflammatory and neuropathic pain.[33,34] To simulate the pain symptoms of BCP, we injected Walker-256 rat mammary gland cancer cells into the tibia of rats. In our experiment, PWT of rats decreased significantly on day 6 after surgery, and continued to decline until the 18th day after operation. Besides, HE staining showed a large variety of larger cell nuclei with heterogeneity and eroded bone trabeculae. Consistent with previous studies,[19,21] these findings indicate that the BCP model has been effectively developed.

Chemokine receptor CXCR1 is a member of the G protein-coupled receptor (GPCR) superfamily. CXCR1 and CXCR2 are involved in neuropathic pain induced by paclitaxel.[35] CXCR2 has been demonstrated to be involved in BCP,[4] while the role of CXCR1 has not yet been investigated. Single-cell RT-PCR showed that the septal neurons containing CXCR1 mRNA responded to IL-8, while CXCR2 mRNA did not, indicating that CXCR1 receptors have certain functions in these neurons.[36] CXCR1 (mRNA and protein) in ipsilateral spinal cord was upregulated under BCP conditions (Figure 3(d)). CXCR1 was highly expressed in the spinal dorsal horn laminae I–V (Figure 3(b)), which is a key site for processing nociceptive information. In this study, we also performed immunofluorescence double staining on CXCR1 with neurons (NeuN), astrocytes (GFAP), and microglia (Iba-1) to investigate location of receptors. The results suggest CXCR1 seemed to predominantly co-localize with neurons. CXCR1 is distributed widely on neurons in the brain regions, such as the expression of GABAergic, cholinergic, and glutamatergic markers.[7]

We inhibited CXCR1 by intrathecal injection of SiRNA to determine the function of CXCR1 receptor in BCP development. Catwalk gait analysis system and Von Frey test evaluated BCP-related behavior.[25,37] We conducted a Catwalk gait analysis system to examine the abnormal features of the affected limbs, when the rats were carrying weight during autonomous walking. In this study, the maximum contact area, mean intensity, and maximum contact intensity declined in tumor-bearing rats, indicating that the weight bearing capacity decreased. The behavioral study also showed that intrathecal siRNA injection could significantly reverse the abnormal gait characteristics caused by tumor. Consistent with this, PWT also increased after intrathecal injection of siRNA (Figure 5(d)). At the same time, CXCR1 protein levels showed a significant decrease (Figure 5(c)).

JAK2/STAT3 signaling pathway is an established tumor and inflammation mechanism.[38,39] In the spinal cord of BCP rats, we noted that the p-JAK2/JAK2 and p-STAT3/STAT3 ratios increased significantly on day 12.[19]. Blocking the JAK2/STAT3 signaling pathway can significantly reduce the mechanical hyperalgesia of BCP.[13] Targeting p-STAT3 may be a feasible method to treat BCP.[40] In BCP model, after

intrathecal injection of CXCR1-siRNA, phosphorylated proteins of JAK2/STAT3 pathway were significantly inhibited. The same results were confirmed in vitro.

NLRP3 inflammasome becomes a target for the prevention and treatment of central nervous system diseases.[41,42] The expression of NLRP3 inflammasome in BCP increased significantly in a time-dependent manner and was mainly co-localized with NeuN in SDH.[43] We found that BCP upregulated NLRP3, IL-1β, and caspase-1 expression in vitro and in vivo. Meanwhile, this effect could be reversed by CXCR1 knockdown by siRNA. Thus, the NLRP3 inflammasome-mediated inflammatory cascade might be a potential target for BCP-induced mechanical hyperalgesia treatment.

Intrathecal injection of JAK2 inhibitor AG-490 attenuated BCP-related mechanical allodynia.[44] Zhang et al.[45] showed that JAK2/STAT3 signaling pathway participated in BCP by upregulating voltage-gated sodium channel activation in neurons. Tian et al. suggested that small molecule inhibitors of NLRP3 MCC950 significantly attenuated BCP-related mechanical allodynia.[43] In our experiment, intrathecal injection of CXCR1-siRNA significantly inhibited the protein expression of JAK2/STAT3 signaling pathway and NLRP3 inflammasome. Based on the above evidence, we speculate that CXCR1 may mediate BCP through JAK2/STAT3 signaling pathway and NLRP3 inflammasome.

Conclusions

We found that the inoculation of Walker 256 cells into the tibia of rats caused pain hypersensitivity and bone destruction. In addition to these changes, the chemokine receptor CXCR1 in spinal dorsal horn neurons increased. Inhibition of CXCR1 receptor can reduce the activation of JAK2/STAT3 signaling pathway and NLRP3 inflammasome. CXCR1 receptor may be a new target for Walker 256 induced BCP treatment.

Author contributions

C.X. and M.Y. performed experiments and analyzed data; L.X., B.Z., M.X., Q.H., C.N., J.F., B.L., M.K. and Y.W. interpreted results of experiments; C.X. and L.X. prepared figures; C.X. and L.X. drafted manuscript; C.X. and M.Y. edited and revised manuscript; M.Y., X.L. and H.N. conceived and designed the research. All authors approved the final version of the manuscript authorship and/or publication of this article.

Declaration of conflicting interests

The author(s) declared no potential conflicts of interest with respect to the research, authorship, and/or publication of this article.

Ethical approval

The animal study was reviewed and approved by Animal Care and Use Committee of Jiaxing University.

Data availability statement

The datasets generated for this study are available on request to the corresponding author.

ORCID iDs

Huadong Ni https://orcid.org/0000-0001-7092-3474
Ming Yao https://orcid.org/0000-0002-4226-8473

References

1. Weilbaecher KN, Guise TA, McCauley LK. Cancer to bone: a fatal attraction. *Nat Rev Cancer* 2011; 11: 411–425. DOI: 10.1038/nrc3055.

2. van den Beuken-van Everdingen MH, Hochstenbach LM, Joosten EA, Tjan-Heijnen VC, Janssen DJ. Update on prevalence of pain in patients with cancer: systematic review and meta-analysis. *J Pain Symptom Manage* 2016; 51: 1070–1090.e9. DOI: 10.1016/j.jpainsymman.2015.12.340.

3. Falk S, Dickenson AH. Pain and nociception: mechanisms of cancer-induced bone pain. *J Clin Oncol* 2014; 32: 1647–1654. DOI: 10.1200/jco.2013.51.7219.

4. Xu J, Zhu MD, Zhang X, Tian H, Zhang JH, Wu XB, Gao YJ. NFκB-mediated CXCL1 production in spinal cord astrocytes contributes to the maintenance of bone cancer pain in mice. *J Neuroinflammation* 2014; 11: 38. DOI: 10.1186/1742-2094-11-38.

5. Lu C, Zhu J, Chen X, Hu Y, Xie W, Yao J, Huang S. Risk stratification in acute myeloid leukemia using CXCR gene signatures: a bioinformatics analysis. *Front Oncol* 2020; 10: 584766. DOI: 10.3389/fonc.2020.584766.

6. Carevic M, Öz H, Fuchs K, Laval J, Schroth C, Frey N, Hector A, Bilich T, Haug M, Schmidt A, Autenrieth SE, Bucher K, Beer-Hammer S, Gaggar A, Kneilling M, Benarafa C, Gao JL, Murphy PM, Schwarz S, Moepps B, Hartl D. CXCR1 regulates pulmonary anti-pseudomonas host defense. *J Innate Immunity* 2016; 8: 362–373. DOI: 10.1159/000444125.

7. Danik M, Puma C, Quirion R, Williams S. Widely expressed transcripts for chemokine receptor CXCR1 in identified glutamatergic, gamma-aminobutyric acidergic, and cholinergic neurons and astrocytes of the rat brain: a single-cell reverse transcription-multiplex polymerase chain reaction study. *J Neurosci Res* 2003; 74: 286–295. DOI: 10.1002/jnr.10744.

8. Cao DL, Zhang ZJ, Xie RG, Jiang BC, Ji RR, Gao YJ. Chemokine CXCL1 enhances inflammatory pain and increases NMDA receptor activity and COX-2 expression in spinal cord neurons via activation of CXCR2. *Exp Neurol* 2014; 261: 328–336. DOI: 10.1016/j.expneurol.2014.05.014.

9. Chen G, Park CK, Xie RG, Berta T, Nedergaard M, Ji RR. Connexin-43 induces chemokine release from spinal cord astrocytes to maintain late-phase neuropathic pain in mice. *Brain* 2014; 137: 2193–2209. DOI: 10.1093/brain/awu140.

10. Meesawatsom P, Hathway G, Bennett A, Constantin-Teodosiu D, Chapman V. Spinal neuronal excitability and neuroinflammation in a model of chemotherapeutic neuropathic pain: targeting the resolution pathways. *J Neuroinflammation* 2020; 17: 316–2020. DOI: 10.1186/s12974-020-01997-w.

11. Yu S, Zhao G, Han F, Liang W, Jiao Y, Li Z, Li L. Muscone relieves inflammatory pain by inhibiting microglial activation-mediated inflammatory response via abrogation of the NOX4/JAK2-STAT3 pathway and NLRP3 inflammasome. *Int Immunopharmacol* 2020; 82: 106355. DOI: 10.1016/j.intimp.2020.106355.

12. Li HN, Yang QQ, Wang WT, Tian X, Feng F, Zhang ST, Xia YT, Wang JX, Zou YW, Wang JY, Zeng XY. Red nucleus IL-33 facilitates the early development of mononeuropathic pain in male rats by inducing TNF-α through activating ERK, p38 MAPK, and JAK2/STAT3. *J Neuroinflammation* 2021; 18: 150. DOI: 10.1186/s12974-021-02198-9.

13. Liu M, Cheng X, Yan H, Chen J, Liu C, Chen Z. MiR-135-5p alleviates bone cancer pain by regulating astrocyte-mediated neuroinflammation in spinal cord through JAK2/STAT3 signaling pathway. *Mol Neurobiol* 2021; 58: 4802–4815. DOI: 10.1007/s12035-021-02458-y.

14. Fu J, Zhao B, Ni C, Ni H, Xu L, He Q, Xu M, Xu C, Luo G, Zhu J, Tao J, Yao M. Rosiglitazone alleviates mechanical allodynia of rats with bone cancer pain through the activation of PPAR-γ to inhibit the NF-κB/NLRP3 Inflammatory Axis in Spinal Cord Neurons. *PPAR Res* 2021; 2021: 6086265. DOI: 10.1155/2021/6086265.

15. Zhou YS, Cui Y, Zheng JX, Quan YQ, Wu SX, Xu H, Han Y. Luteolin relieves lung cancer-induced bone pain by inhibiting NLRP3 inflammasomes and glial activation in the spinal dorsal horn in mice. *Phytomedicine* 2022; 96: 153910. DOI: 10.1016/j.phymed.2021.153910.

16. Zhu H, Jian Z, Zhong Y, Ye Y, Zhang Y, Hu X, Pu B, Gu L, Xiong X. Janus kinase inhibition ameliorates ischemic stroke injury and neuroinflammation through reducing NLRP3 inflammasome activation via JAK2/STAT3 pathway inhibition. *Front Immunol* 2021; 12: 714943. DOI: 10.3389/fimmu.2021.714943.

17. Zimmermann M. Ethical guidelines for investigations of experimental pain in conscious animals. *Pain* 1983; 16: 109–110. DOI: 10.1016/0304-3959(83)90201-4.

18. He Q, Wang T, Ni H, Liu Q, An K, Tao J, Chen Y, Xu L, Zhu C, Yao M. Endoplasmic reticulum stress promoting caspase signaling pathway-dependent apoptosis contributes to bone cancer

pain in the spinal dorsal horn. *Mol Pain* 2019; 15: 1744806919876150. DOI: 10.1177/1744806919876150.

19. Xu M, Ni H, Xu L, Shen H, Deng H, Wang Y, Yao M. B14 ameliorates bone cancer pain through downregulating spinal interleukin-1β via suppressing neuron JAK2/STAT3 pathway. *Mol Pain* 2019; 15: 1744806919886498. DOI: 10.1177/1744806919886498.

20. Gabriel AF, Marcus MA, Walenkamp GH, Joosten EA. The CatWalk method: assessment of mechanical allodynia in experimental chronic pain. *Behav Brain Res* 2009; 198: 477–480. DOI: 10.1016/j.bbr.2008.12.018.

21. Fu J, Ni C, Ni HD, Xu LS, He QL, Pan H, Huang DD, Sun YB, Luo G, Liu MJ, Yao M. Spinal Nrf2 translocation may inhibit neuronal NF-κB activation and alleviate allodynia in a rat model of bone cancer pain. *J Neurochem* 2021; 158: 1110–1130. DOI: 10.1111/jnc.15468.

22. Li TF, Wu HY, Wang YR, Li XY, Wang YX. Molecular signaling underlying bulleyaconitine A (BAA)-induced microglial expression of prodynorphin. *Sci Rep* 2017; 7: 45056. DOI: 10.1038/srep45056.

23. Mao-Ying QL, Zhao J, Dong ZQ, Wang J, Yu J, Yan MF, Zhang YQ, Wu GC, Wang YQ. A rat model of bone cancer pain induced by intra-tibia inoculation of Walker 256 mammary gland carcinoma cells. *Biochem Biophys Res Commun* 2006; 345: 1292–1298. DOI: 10.1016/j.bbrc.2006.04.186.

24. Xu H, Peng C, Chen XT, Yao YY, Chen LP, Yin Q, Shen W. Chemokine receptor CXCR4 activates the RhoA/ROCK2 pathway in spinal neurons that induces bone cancer pain. *Mol Pain* 2020; 16: 1744806920919568. DOI: 10.1177/1744806920919568.

25. Hu XM, Yang W, Du LX, Cui WQ, Mi WL, Mao-Ying QL, Chu YX, Wang YQ. Vascular endothelial growth factor a signaling promotes spinal central sensitization and pain-related behaviors in female rats with bone cancer. *Anesthesiology* 2019; 131: 1125–1147. DOI: 10.1097/aln.0000000000002916.

26. Cui S, Zhu Y, Du J, Khan MN, Wang B, Wei J, Cheng JW, Gordon JR, Mu Y, Li F. CXCL8 antagonist improves diabetic nephropathy in male mice with diabetes and attenuates high glucose-induced mesangial injury. *Endocrinology* 2017; 158: 1671–1684. DOI: 10.1210/en.2016-1781.

27. Han XG, Du L, Qiao H, Tu B, Wang YG, Qin A, Dai KR, Fan QM, Tang TT. CXCR1 knockdown improves the sensitivity of osteosarcoma to cisplatin. *Cancer Letters* 2015; 369: 405–415. DOI: 10.1016/j.canlet.2015.09.002.

28. Kim SJ, Park SM, Cho YW, Jung YJ, Lee DG, Jang SH, Park HW, Hwang SJ, Ahn SH. Changes in expression of mRNA for interleukin-8 and effects of interleukin-8 receptor inhibitor in the spinal dorsal horn in a rat model of lumbar disc herniation. *Spine (Phila Pa 1976)* 2011; 36: 2139–2146. DOI: 10.1097/BRS.0b013e31821945a3.

29. Ruan Y, Ling J, Ye F, Cheng N, Wu F, Tang Z, Cheng X, Liu H. Paeoniflorin alleviates CFA-induced inflammatory pain by inhibiting TRPV1 and succinate/SUCNR1-HIF-1α/NLPR3 pathway. *Int Immunopharmacol* 2021; 101: 108364. DOI: 10.1016/j.intimp.2021.108364.

30. Derangula K, Javalgekar M, Kumar Arruri V, Gundu C, Kumar Kalvala A, Kumar A. Probucol attenuates NF-κB/NLRP3 signalling and augments Nrf-2 mediated antioxidant defence in nerve injury induced neuropathic pain. *Int Immunopharmacol* 2022; 102: 108397. DOI: 10.1016/j.intimp.2021.108397.

31. Schloss J, Ryan K, Steel A. Corrigendum to a randomised, double-blind, placebo-controlled clinical trial found that a novel herbal formula UROX® BEDTIME BUDDY assisted children for the treatment of nocturnal enuresis. Phytomedicine (2021) 153783 https://doi.org/10.1016/j.phymed.2021.153783. *Phytomedicine* 2022; 99: 153992. DOI: 10.1016/j.phymed.2022.153992.

32. Ye Y, Zhang Y, Wang B, Walana W, Wei J, Gordon JR, Li F. CXCR1/CXCR2 antagonist G31P inhibits nephritis in a mouse model of uric acid nephropathy. *Biomed Pharmacother* 2018; 107: 1142–1150. DOI: 10.1016/j.biopha.2018.07.077.

33. Yang B, Zhang Z, Yang Z, Ruan J, Luo L, Long F, Tang D. Chanling Gao attenuates bone cancer pain in rats by the IKKβ/NF-κB signaling pathway. *Front Pharmacol* 2020; 11: 525–2020. DOI: 10.3389/fphar.2020.00525.

34. Kong X, Wei J, Wang D, Zhu X, Zhou Y, Wang S, Xu GY, Jiang GQ. Upregulation of spinal voltage-dependent anion channel 1 contributes to bone cancer pain hypersensitivity in rats. *Neurosci Bull* 2017; 33: 711–721. DOI: 10.1007/s12264-017-0195-1.

35. Carreira EU, Carregaro V, Teixeira MM, Moriconi A, Aramini A, Verri WA Jr, Ferreira SH, Cunha FQ, Cunha TM. Neutrophils recruited by CXCR1/2 signalling mediate post-incisional pain. *Eur J Pain* 2013; 17: 654–663. DOI: 10.1002/j.1532-2149.2012.00240.x.

36. Puma C, Danik M, Quirion R, Ramon F, Williams S. The chemokine interleukin-8 acutely reduces Ca(2+) currents in identified cholinergic septal neurons expressing CXCR1 and CXCR2 receptor mRNAs. *J Neurochem* 2001; 78: 960–971. DOI: 10.1046/j.1471-4159.2001.00469.x.

37. Hu S, Mao-Ying QL, Wang J, Wang ZF, Mi WL, Wang XW, Jiang JW, Huang YL, Wu GC, Wang YQ. Lipoxins and aspirin-triggered lipoxin alleviate bone cancer pain in association with suppressing expression of spinal proinflammatory cytokines. *J Neuroinflammation* 2012; 9: 278–2012. DOI: 10.1186/1742-2094-9-278.

38. Yuan K, Ye J, Liu Z, Ren Y, He W, Xu J, He Y, Yuan Y. Complement C3 overexpression activates JAK2/STAT3 pathway and correlates with gastric cancer progression. *J Exp Clin Cancer Res* 2020; 39: 9. DOI: 10.1186/s13046-019-1514-3.

39. Yu L, Zhang Y, Chen Q, He Y, Zhou H, Wan H, Yang J. Formononetin protects against inflammation associated with cerebral ischemia-reperfusion injury in rats by targeting the JAK2/STAT3 signaling pathway. *Biomed Pharmacother* 2022; 149: 112836. DOI: 10.1016/j.biopha.2022.112836.

40. Linher-Melville K, Sharma M, Nakhla P, Kum E, Ungard R, Park J, Rosa D, Gunning P, Singh G. Inhibiting STAT3 in a murine model of human breast cancer-induced bone pain delays the onset of nociception. *Mol Pain* 2019; 15: 1744806918823477. DOI: 10.1177/1744806918823477.

41. Liu SB, Mi WL, Wang YQ. Research progress on the NLRP3 inflammasome and its role in the central nervous system. *Neurosci Bull* 2013; 29: 779–787. DOI: 10.1007/s12264-013-1328-9.

42. Wang S, He H, Long J, Sui X, Yang J, Lin G, Wang Q, Wang Y, Luo Y. TRPV4 regulates soman-induced status epilepticus and secondary brain injury via NMDA receptor and NLRP3 inflammasome. *Neurosci Bull* 2021; 37: 905–920. DOI: 10.1007/s12264-021-00662-3.

43. Chen SP, Zhou YQ, Wang XM, Sun J, Cao F, HaiSam S, Ye DW, Tian YK. Pharmacological inhibition of the NLRP3 inflammasome as a potential target for cancer-induced bone pain.

Pharmacol Res 2019; 147: 104339. DOI: 10.1016/j.phrs.2019.104339.

44. Zhang J, Ren B, Ni K, Liu Y, Ma Z. [Intrathecal injection of AG-490 reduces bone-cancer-induced spinal cord astrocyte reaction and thermal hyperalgesia in a mouse model]. *Zhong Nan Da Xue Xue Bao Yi Xue Ban* 2018; 43: 1182–1187. DOI: 10.11817/j.issn.1672-7347.2018.11.003.

45. Zhang F, Wang Y, Liu Y, Han H, Zhang D, Fan X, Du X, Gamper N, Zhang H. Transcriptional regulation of voltage-gated sodium channels contributes to GM-CSF-induced pain. *J Neurosci* 2019; 39: 5222–5233. DOI: 10.1523/jneurosci.2204-18.2019.